

## Supporting Information

# Imaging Metastasis Using an Integrin-Targeting Chain-Shaped Nanoparticle

Pubudu M. Peiris<sup>1, 2, 3</sup>, Randall Toy<sup>1, 3</sup>, Elizabeth Doolittle<sup>1, 3</sup>, Jenna Pansky<sup>1, 3</sup>, Aaron Abramowski<sup>1, 3</sup>, Morgan Tam<sup>1, 3</sup>, Peter Vicente<sup>1, 3</sup>, Emily Tran<sup>1, 3</sup>, Elliott Hayden<sup>1, 3</sup>, Andrew Camann<sup>1, 3</sup>, Aaron Mayer<sup>1, 3</sup>, Bernadette O. Erokwu<sup>2, 3</sup>, Zachary Berman<sup>2, 3</sup>, David Wilson<sup>1, 3, 4</sup>, Harihara Baskaran<sup>4, 5</sup>, Chris A. Flask<sup>1, 2, 3, 4</sup>, Ruth A. Keri<sup>4, 6</sup>, and Efstathios Karathanasis<sup>1, 2, 3, 4, \*</sup>

<sup>1</sup> Department of Biomedical Engineering, Case Western Reserve University, Cleveland, Ohio

<sup>2</sup> Department of Radiology, Case Western Reserve University, Cleveland, Ohio

<sup>3</sup> Case Center for Imaging Research, Case Western Reserve University, Cleveland, Ohio

<sup>4</sup> Case Comprehensive Cancer Center, Case Western Reserve University, Cleveland, Ohio

<sup>5</sup> Department of Chemical Engineering, Case Western Reserve University, Cleveland, Ohio

<sup>6</sup> Department of Pharmacology, Case Western Reserve University, Cleveland, Ohio

\* Author to whom correspondence should be addressed: Efstathios Karathanasis  
email: [stathis@case.edu](mailto:stathis@case.edu)

## Contents

Supporting Figure S1: TEM image shows a nanochain

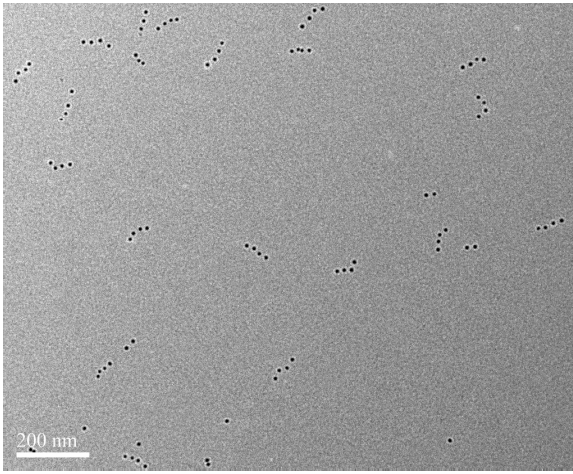
Supporting Figure S2: *In vitro* targeting of endothelial cells under static and flow conditions

Supporting Results: *In vitro* targeting of nanochains under static and flow conditions

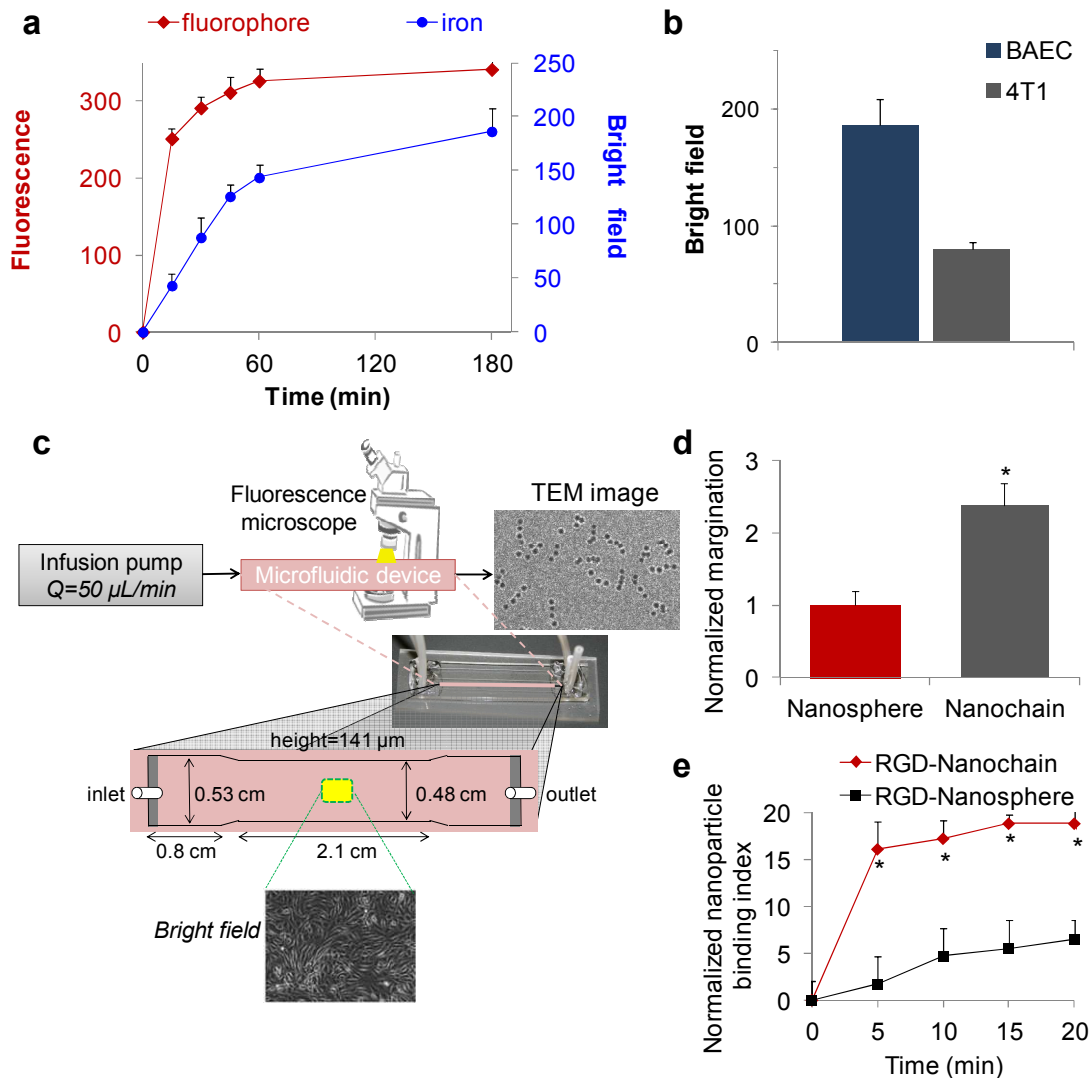
Supporting Methods: Synthesis and characterization of iron oxide nanospheres with asymmetric surface chemistry

Supporting Methods: Synthesis and characterization of nanochains

Supporting Methods: *In vitro* targeting



**Supporting Figure S1.** TEM image shows a nanochain prior to conjugation of the RGD peptide. The nanochains predominantly composed of four IO spheres.



**Supporting Figure S2.** *In vitro* targeting of integrin-expressing endothelial cells under static and flow conditions. (a) After treatment of BAEC cells with  $\text{TNF-}\alpha$ , the cells were incubated with an excess of RGD-NC nanoparticles for 15, 30, 45, 60 and 180 min ( $n=3$  for each time point). The cells were fixed and stained for iron using Prussian blue. Representative bright field images are shown. Quantification of

the signal in fluorescence and bright field images provided the time course of RGD-NC targeting. **(b)** Comparison of the cellular uptake of RGD-NC nanoparticles by BAEC and 4T1 cells after 3 h of incubation with the nanoparticles. **(c)** Schematic of the microfluidic experimental setup. The TEM image shows the nanochain suspension in cell culture media after the particles were flowed at 50  $\mu\text{L}/\text{min}$  for 20 min. **(d)** The margination of the nanospheres and nanochains was compared in a fibronectin-coated microchannel. At  $t < 0$ , the microchannel was filled with PBS. At  $t = 2.15 \times 10^{12}$  nanoparticles/mL were flowed through the microchannel at 50  $\mu\text{L}/\text{min}$ . At  $t = 10$  min, the lumen was flushed with PBS. The nanoparticles deposited in the microchannel were collected by an ethanol flush. Those collections were quantified with a fluorescence reader which was the basis of the quantitative analysis. **(e)** The targeting avidity of the nanospheres and nanochains was evaluated under flow conditions in microchannel seeded with BAEC cells. A series of 12-bit images were captured using a fluorescence microscope which enabled the dynamic quantitative analysis showed in the plot. At  $t < 0$ , the microchannel was filled with the cell culture media. RGD-NC nanoparticles or RGD-targeted nanosphere with the same concentration of particle/mL were flowed through the microchannel at 50  $\mu\text{L}/\text{min}$  ( $n=4$  per conditions).

### Supporting Results: *In vitro* targeting of nanochains under static and flow conditions

We evaluated the binding dynamics of the RGD-NC nanoparticles to integrin-expressing endothelial cells *in vitro* under static and flow conditions. After treating bovine aortic endothelial cells (BAEC) with  $\text{TNF-}\alpha$  to induce expression of  $\alpha_v\beta_3$  integrins,<sup>1</sup> the cells were incubated with an excess of RGD-NC nanoparticles for different periods of time. After the cells were washed, fixed and stained for iron (Prussian blue), bright field (for iron) and fluorescence (for the fluorescent tag) images were obtained to quantitatively assess the uptake of the nanoparticles. Figure S2a shows the time course of the nanoparticle uptake by the cells. The profile exhibits a sharp increase in the first 60 min followed by a slower uptake rate. Notably, the fluorescence-based measurements indicated the nanoparticle uptake peaked at about 45 min followed by a plateau in the later time points, which suggests that quenching of the intracellular fluorescence signal occurred at the higher nanoparticle concentrations. In addition, Figure S2b compares the uptake of the RGD-NC particles by  $\text{TNF-}\alpha$ -treated BAEC and 4T1 cells after 3 h of incubation. While the endothelial cells exhibited higher cellular uptake, the 4T1 cells showed that they were targetable by an integrin-targeted nanoparticle.

We evaluated the ability of the RGD-NC particle to perform vascular targeting in microcirculation using our previously established *in vitro* method in a microfluidic device.<sup>2</sup> Figure S2c shows a schematic of the experimental setup. The device consisted of a straight microchannel with dimensions of 3.5 x 0.48 cm (length x width) and height of 114  $\mu\text{m}$ . We separately measured the margination rates and avidity of the nanochains. Firstly, the margination rates of non-targeted IO nanochains and nanospheres were evaluated. To capture marginating nanoparticles in a broad non-specific manner, the surface of the microchannel was coated with fibronectin overnight.<sup>2</sup> The nanoparticle suspension was infused *via* a syringe pump into microchannel filled with culture media at a flow rate of 50  $\mu\text{L}/\text{min}$ , which is in the range of expected blood flow in the tumor microcirculation.<sup>3</sup> The nanoparticles were allowed to run through the system for 10 min followed by PBS flushing and finally ethanol wash to completely collect the deposited nanoparticles from the channel. The channel was semi-quantitatively monitored in real-time using fluorescence microscopy as before. Upon collection of only the wall-deposited nanoparticles using a final ethanol wash, the deposition of the nanoparticles was quantified using a fluorescence reader. The nanochain exhibited 2.3-fold higher margination than the IO sphere (Figure S2d).

Targeting avidity of the RGD-NC particle was also assessed under flow using the microfluidic device coated with  $\text{TNF-}\alpha$ -treated BAEC cells. BAEC cells were seeded onto fibronectin-coated microchannels (bright field image in Figure S2c) and treated with  $\text{TNF-}\alpha$ . Fluorescence microscopy was used to quantitatively evaluate in real time the binding of the fluorescently tagged nanoparticles to BAEC cells on the channel. It should be noted that the concentration of the nanoparticle suspension was equal for

both the nanochains and nanospheres ( $2.15 \times 10^{12}$  particles/mL). In addition, both types of nanoparticles contained approximately the same number of fluorophore tags per particle. Figure S2e compares the adhesive strength of RGD-nanochains to RGD-nanospheres. Both nanoparticles displayed a biphasic behavior comprising of an initial rapid attachment phase followed by a slower attachment rate. Notably, after 5 and 20 min, the RGD-NC nanoparticles achieved 9.5 and 2.9-fold higher attachment compared to their spherical counterparts. Furthermore, it should be noted that both the chain-shaped and spherical nanoparticles used in this study displayed a very mild charge (about -10 mV). Therefore, the nanoparticle deposition on the channel could not be attributed to ionic interactions.

### **Supporting Methods: Synthesis and characterization of iron oxide nanospheres with asymmetric surface chemistry**

Solid-phase chemistry was used to partially modify the surface functionality of iron oxide nanospheres (Ocean Nanotech). The iron oxide nanospheres were prepared using iron oxide powder as the iron precursor, oleic acid as the ligand, and octadecene as the solvent.<sup>2,3</sup> The particles were coated with a triblock polymer consisting of polybutylacrylate segment (hydrophobic), polymethacrylic acid (hydrophilic) and a hydrophobic carbon side chain. Amine-terminated polyethylene glycol polymer was conjugated onto the carboxyl groups of the surface of iron oxide nanoparticles. CLEAR (Cross-Linked Ethoxylate Acrylate Resin) resin (Peptides International Inc, Louisville, KY) with different densities of amine functional group, was used as solid support. CLEAR resin (250 mg) was placed in a fritted reactor and was washed and swollen in DMF followed by PBS. The homobifunctional cleavable cross-linkers 3,3'-Dithiobis(sulfosuccinimidylpropionate) (0.32 mmol, DTSSP; Thermo Scientific, Rockford, IL) was introduced and allowed to react for 15 min. After the washing/drying cycle to remove unbound DTSSP, 1 mL of amine functionalized iron oxide nanospheres at 1 mg/mL iron concentration was added and mixed with the resin beads. The conjugation reaction was allowed to proceed for 45 min with shaking. The nanosphere-resin complex was filtered and a washing/drying cycle was carried out to remove unbound nanospheres. Tris[2-carboxyethyl] phosphine (1.8 mmol, TCEP), a reducing agent, was added and kept for 1-3 hours to cleave off the nanospheres from the resin. The suspension of iron oxide nanospheres with Asymmetric Surface Chemistry (ASC) was collected and dialyzed in 2000 Da MWCO membrane against PBS to remove the excess cleaving reagents.

TEM images were obtained using a Tecnai F30 instrument (FEI, Hillsboro, OR) operated at 300 kV. The sample was prepared by dropping 3  $\mu$ L of the nanosphere suspension onto a 400-mesh formvar carbon-coated copper grid, then the excess solution was blotted with a filter paper and the residual wetting layer was allowed to dry in air. The sizes and zeta potentials of the nanospheres were determined using a ZetaPALS dynamic light scattering system (Brookhaven Instruments, Holtsville, NY). The concentration of iron was determined *via* ICP-OES (Optima 7000 DV; Perkin-Elmer, Waltham, MA).

To determine the number of functional groups of each type, the amines on the nanosphere surface were reacted with the Alexa Fluor 488 NHS ester (Invitrogen, Carlsbad, CA). The amount of Alexa 488 on the surface of the nanospheres was analyzed by the fluorescence intensity using a fluorescence plate reader (Synergy HT; BioTek Instruments). In a typical experiment, iron oxide nanospheres with ASC (surface thiols and amines) and their parent iron oxide nanospheres (only surface amines) were incubated with 10 molar excess of NHS-functionalized Alexa Fluor 488 over the surface amines for 2 hours in the dark with stirring. Each suspension was dialyzed against PBS using a 2000 Da MWCO membrane to remove unbound fluorescent tags. The purified solutions were pipetted into a 96-well plate and the intensity of the fluorescence signal was measured (excitation 480 nm, emission 520 nm). The exact iron concentration was assessed by ICP-OES after digesting all samples with concentrated HNO<sub>3</sub> acid. It was converted to particle concentration with the assumption that each particle was made of Fe<sub>3</sub>O<sub>4</sub> and a 5.2 g/cm<sup>3</sup> density.

## Supporting Methods: Synthesis and characterization of nanochains

Solid-phase chemistry was used to synthesize RGD-NC nanoparticles. Initially, 250 mg of amine-functionalized CLEAR resin were reacted with DTSSP (0.32 mmol) for 15 min. After the washing/drying cycle to remove unbound DTSSP, 1 mL of nanospheres with ASC at 50 µg/mL iron concentration and ~ 20 nm in size were added and mixed with resin beads. The conjugation reaction was allowed to proceed for 15 min with shaking. Nanosphere-attached resin was filtered and a washing/drying cycle was carried out to remove unbound particles. An excess amount of sulfo-NHS acetate was introduced and kept for 15 min to block the unreacted amine groups. The heterobifunctional crosslinker, sulfosuccinimidyl 4-[N-maleimidomethyl]cyclohexane-1-carboxylate (0.05 mmol, Sulfo-SMCC) was introduced and kept for 15 min. After removing excess crosslinker, the next wave of nanospheres with ASC was introduced. This process was repeated until the desired length of the nanochain was obtained. Finally, to cleave off the nanochain from the resin, TCEP were added and kept for 1-3 hours. The nanochain suspension was collected and dialyzed in 2000 Da MWCO membrane against PBS to remove the excess cleaving reagents.

TEM analysis was carried out as described previously. The exact iron concentration of the RGD-NC particles was assessed by ICP-OES after digesting all samples with concentrated HNO<sub>3</sub> acid.

## Supporting Methods: *In vitro* targeting

Cellular uptake studies were performed by seeding the BAEC cells at a density of  $2 \times 10^5$  cells/well in 6-well plate 24 h before incubation with the nanoparticles. Prior to incubation, cells were washed three times with fresh medium and then incubated with the RGD-NC nanoparticles for 15, 30, 45, 60 and 180 minutes at a concentration of  $1.3 \times 10^{11}$  particles/mL. At the end of each incubation time, the cells were washed three times with fresh medium, fixed with paraformaldehyde, stained with Prussian blue, and imaged using fluorescence and bright field microscopy. Quantification of the signals were used as a measure of the intracellular content of nanoparticles. Under identical conditions, cellular uptake experiments were also performed with the 4T1 cells.

For the margination experiments under flow conditions, PDMS microchannel devices were incubated with fibronectin at 100 µg/mL overnight. Channels with fibronectin were flushed thoroughly with PBS before the start of the experiment. Fluorescent images of the channel were acquired before the introduction of nanoparticles. Then, nanoparticles at a concentration of  $2.15 \times 10^{12}$  particles/mL were infused into the microchannels with a Harvard syringe pump (Harvard Apparatus, Holliston, MA) at a flow rate of 50 µL/min. Following nanoparticle flow, channels were washed with PBS at a flow rate of 50 µL/min for 30 minutes. Images were acquired in each phase to qualitatively assess particle deposition during the experiment. The non-adherent nanoparticles were collected from the outlet of the microchannel during both the nanoparticle flow and PBS wash phase of the experiment. Adherent nanoparticles were collected separately by flushing the system with ethanol. Particle concentration was measured using a fluorescent plate reader. The volumes of the collected nanoparticles were measured so that the number of adherent and non-adherent nanoparticles could be calculated from mass balance. Percent deposition was then calculated by dividing the total number of adherent nanoparticles by the sum of the number of adherent and non-adherent nanoparticles, multiplied by 100. It should be noted that we performed pilot studies to evaluate potential photobleaching of the fluorophore and whether this should be taken into account. Photobleaching of the Alexa fluorophore was assessed by analyzing images of a channel filled with fluorescently-tagged nanoparticles under static conditions (no flow), exposed continuously to light from the microscope, acquired over a 20 minute time period. It was found that the fluorescence decreased approximately 1% per minute of direct light exposure. In each microchannel experiment, overall image acquisition time was less than 2 minutes. Since quantification of the nanoparticle deposition rates were based on the collection of a large number of particles from the entire channel, the effect of photobleaching on the fluorescence measurements was considered negligible.

For the targeting avidity experiments under flow, PDMS microchannel devices were incubated for 2 h with fibronectin overnight before cell seeding. A BAEC cell suspension was prepared by harvesting cells from a culture flask with trypsin solution, pelleting the cells by centrifugation (300 g, 5 min), removing the supernatant, and resuspending in culture media. This cell suspension was pipetted into the microchannel, and incubated at 37°C and 5% CO<sub>2</sub>. Once the microchannel's surface was covered by endothelial cells, the cells were treated with TNF- $\alpha$  for 2 h. The nanoparticles at a concentration of  $1.3 \times 10^{11}$  particles/mL were infused into the microchannels with a Harvard syringe pump at a flow rate of 50  $\mu$ L/min. Image acquisition was performed using an Olympus IX-71 inverted fluorescent microscope (Olympus). All acquired images were 12-bit grayscale and taken at 20X magnification. Fluorescent images of the channel were acquired before and every 5 min after the introduction of nanoparticles. Fluorescence signal was quantified by determining the average pixel value of an ROI drawn around one segment in the center of the microchannel (as shown in Figure S1b). We confirmed that negligible photobleaching of the fluorescently tagged nanoparticles occurred with the acquisition parameters of the microscope.

## References

1. Gao, B.; Saba, T. M.; Tsan, M. F., Role of Alpha(V)Beta(3)-Integrin in Tnf-Alpha-Induced Endothelial Cell Migration. *Am J Physiol Cell Physiol* 2002, 283, C1196-205.
2. Peiris, P. M.; Schmidt, E.; Calabrese, M.; Karathanasis, E., Assembly of Linear Nano-Chains from Iron Oxide Nanospheres with Asymmetric Surface Chemistry. *PLoS One* 2011, 6, e15927.
3. Yang, L.; Peng, X.; Wang, A.; Wang, X.; Cao, Z.; Ni, C.; karna, P.; Zhang, X.; Wood, W. C.; Gao, X.; Nie, S.; Mao, H., Receptor-Targeted Nanoparticles for *in vivo* Imaging of Breast Cancer. *Clinical Cancer Research* 2009, 15, 4722-4732.